

Constraints on anomalous tcZ coupling from

$\bar{B} \rightarrow \bar{K}^* \mu^+ \mu^-$ and $B_s \rightarrow \mu^+ \mu^-$ decays

Hui Gong¹, Ya-Dong Yang^{1,2} and Xing-Bo Yuan^{1,2}

¹Institute of Particle Physics, Central China Normal University, Wuhan, Hubei 430079, P. R. China

²Key Laboratory of Quark & Lepton Physics, Ministry of Education, Central China Normal University,

Wuhan, Hubei 430079, P. R. China

Abstract

In this paper, we analyze the possible anomalous tcZ coupling effects in the $b \rightarrow s$ mediated decays $\bar{B} \rightarrow \bar{K}^* \mu^+ \mu^-$ and $B_s \rightarrow \mu^+ \mu^-$. After exploiting the available experimental data, the combined constraints on the anomalous coupling X_{ct}^L are derived. It is found that, the bound on the magnitude $|X_{ct}^L|$ is dominated by the branching ratios of these two decays. Furthermore, one sign-flipped solution is excluded by the longitudinal fraction of $\bar{B} \rightarrow \bar{K}^* \mu^+ \mu^-$ at the low dilepton mass region. After considering the combined constraints, for general complex coupling X_{ct}^L , the predicted upper bound on $\mathcal{B}(t \rightarrow cZ)$ are compatible with that from the recent CMS direct search. In particular, for the case of real coupling X_{ct}^L , the upper bound reads $\mathcal{B}(t \rightarrow cZ) < 6.3 \times 10^{-5}$, which is much lower than the current CMS bound but still accessible at the LHC. With improved measurements at the LHC, the closer correlations between the $t \rightarrow cZ$ and $b \rightarrow s$ mediated (semi-) leptonic decays are expected in the near future.

1 Introduction

In the Standard Model (SM), the flavor-changing neutral current (FCNC) transitions are forbidden at tree level and highly suppressed at one-loop level due to the Glashow-Iliopoulos-Maiani (GIM) mechanism [1]. Such processes may receive competing contributions from possible new physics (NP) beyond the SM, as a result of which the expected rates related to these processes can be significantly altered. Thus the FCNC processes are promising probes of the SM and its extensions.

For the top quark in particular, the FCNC decays $t \rightarrow qZ$ (where q denotes a c - or u -flavored quark) are predicted to be far below the detectable level within the SM, with branching ratios of order of 10^{-10} [2, 3]. However, there are various NP models that may enhance these processes significantly [4, 5]. This makes any positive signal of these decays an indirect evidence of NP beyond the SM. Search for the top quark FCNC decays has been performed at the Tevatron [6, 7] and the LHC [8, 9]. The best upper limits on branching ratio of $\mathcal{B}(t \rightarrow qZ) < 0.24\%$ at 95% C.L. are recently established by the CMS collaboration [9]. Improved direct searches will be available at the LHC due to its large top sample in prospect. The discovery potential of $\mathcal{B}(t \rightarrow qZ)$ is of the order 10^{-4} at the ATLAS [10, 11] and the CMS [12].

However, when studying the phenomena of the $t \rightarrow qZ$ transition, or equivalently an effective anomalous tqZ coupling, at high-energy colliders, the low-energy processes involving the top quark loops should also be taken into account [13–21]. In our previous works [22–24], we have investigated the top quark anomalous coupling effects in rare B and K-meson decays. For the anomalous tcZ coupling in particular, it is found that the dominant constraints come from the $B_s \rightarrow \mu^+\mu^-$ decay. As another $b \rightarrow s\mu^+\mu^-$ process, the $\bar{B} \rightarrow \bar{K}^*\mu^+\mu^-$ decay has been investigated in the literature [25–30] and shown to be able to provide complementary information about the potential NP contributions [31–35]. Its subsequent $K^* \rightarrow K\pi$ processes allow to offer a large number of observables in the fully differential distribution through an angular analysis of the $K\pi\mu^+\mu^-$ final state [36, 37]. Furthermore, the hadronic uncertainties in some angular observables cancel each other, which makes theoretical predictions precise [38, 39]. On the experimental side, the $\bar{B} \rightarrow \bar{K}^*\mu^+\mu^-$ decays have been measured by the experiments BaBar [40], Belle [41], CDF [42, 43] and LHCb (with an integrated luminosity of 0.37 fb^{-1}) [44]. In the near future the LHCb collaboration expects to improve these measurements by using an

integrated luminosity of 1.5 fb^{-1} data [45].

Recently, the first evidence for the decay $B_s \rightarrow \mu^+ \mu^-$ has been announced by the LHCb collaboration [46]. The observed rate $\mathcal{B}(B_s \rightarrow \mu^+ \mu^-) = (3.2_{-1.2}^{+1.5}) \times 10^{-9}$ is in good agreement with the SM prediction. In this paper, motivated by the LHCb result, we shall update the bound on the anomalous tcZ coupling obtained in our previous work [24] with this recent data. After performing a model-independent study of the anomalous tcZ coupling effects in the $\bar{B} \rightarrow \bar{K}^* \mu^+ \mu^-$ decays, we derive the combined bounds on its strength by these two decay modes. The implications for the direct search of the rare $t \rightarrow cZ$ decays at the LHC are also discussed.

Our paper is organized as follows: In section 2, we introduce the effective Lagrangian describing the anomalous tqZ interactions. Section 3 gives a short review on the $B_s \rightarrow \mu^+ \mu^-$ and $\bar{B} \rightarrow \bar{K}^* \mu^+ \mu^-$ decays and also the anomalous tcZ coupling effects in these two decays. In section 4, we give our detailed numerical results and discussions. We conclude in section 5. The relevant formulae for our analysis are shown in the Appendices.

2 Effective Lagrangian for anomalous tqZ couplings

From the viewpoint of effective field theory, the SM can be considered as an effective low-energy theory of an underlying theory at a scale Λ which is much higher than the electroweak scale $v = 246 \text{ GeV}$ [47]. The NP effects above the electroweak scale can be encoded in the higher dimensional interaction terms involving only the SM fields and invariant under the SM gauge symmetry. In particular, the FCNC transitions $t \rightarrow qZ$ can be described by a few dimension 6 operators [48, 49]. These operators can contribute to the tqZ vertices, resulting an equivalent description by the effective Lagrangian [48, 50, 51]

$$\begin{aligned} \mathcal{L}_{tqZ} = & + \frac{g}{2 \cos \theta_W} \bar{q} \gamma^\mu (X_{qt}^L P_L + X_{qt}^R P_R) t Z_\mu \\ & + \frac{g}{2 \cos \theta_W} \bar{q} \frac{i \sigma^{\mu\nu} p_\nu}{m_Z} (\kappa_{qt}^L P_L + \kappa_{qt}^R P_R) t Z_\mu + \text{h.c.}, \end{aligned} \quad (2.1)$$

with $P_{L,R} = (1 \mp \gamma^5)/2$. The dimensionless couplings $X_{qt}^{L,R}$ and $\kappa_{qt}^{L,R}$ are complex generally and can be written in terms of its magnitude and phase as, for example, $X_{ct}^L \equiv |X_{ct}^L| e^{i\theta_{ct}^L}$. This Lagrangian has been employed in phenomenological analyses related to top-quark physics [4, 5].

3 Theoretical Framework

In this section, we shall first introduce the theoretical framework of the $B_s \rightarrow \mu^+\mu^-$ and $\bar{B} \rightarrow \bar{K}^*l^+l^-$ decays, and then discuss the anomalous tqZ coupling effects in these two decays.

3.1 Effective Hamiltonian

In the SM, the effective Hamiltonian for the $b \rightarrow sl^+l^-$ transitions read [52, 53]

$$\mathcal{H}_{\text{eff}} = -\frac{4G_F}{\sqrt{2}} \left(\lambda_t \mathcal{H}_{\text{eff}}^{(t)} + \lambda_u \mathcal{H}_{\text{eff}}^{(u)} \right), \quad (3.1)$$

with the products of the CKM matrix elements $\lambda_q \equiv V_{qb}V_{qs}^*$ and

$$\mathcal{H}_{\text{eff}}^{(t)} = C_1 \mathcal{O}_1^c + C_2 \mathcal{O}_2^c + \sum_{i=3}^{10} C_i \mathcal{O}_i, \quad \mathcal{H}_{\text{eff}}^{(u)} = C_1 (\mathcal{O}_1^c - \mathcal{O}_2^u) + C_2 (\mathcal{O}_2^c - \mathcal{O}_2^u), \quad (3.2)$$

where the explicit expressions of \mathcal{O}_{1-6} can be found in ref. [52, 53]. The Wilson coefficients, which contain the short-distance physics, can be calculated perturbatively at the high scale $\mu = \mu_W$. At the low scale $\mu = \mu_b$, their values are obtained by means of QCD renormalization group equations, which has been performed at NNLL accuracy [53–56]. For the $B_s \rightarrow \mu^+\mu^-$ and $\bar{B} \rightarrow \bar{K}^*l^+l^-$ decays, the electromagnetic dipole operator and semileptonic four-fermion operators are more relevant [25]

$$\mathcal{O}_7 = \frac{e}{g_s^2} m_b (\bar{s} \sigma_{\mu\nu} P_R b) F^{\mu\nu}, \quad \mathcal{O}_9 = \frac{e^2}{g_s^2} (\bar{s} \gamma_\mu P_L b) (\bar{l} \gamma^\mu l), \quad \mathcal{O}_{10} = \frac{e^2}{g_s^2} (\bar{s} \gamma_\mu P_L b) (\bar{l} \gamma^\mu \gamma_5 l), \quad (3.3)$$

where g_s is the strong coupling constant. The remaining operators enter the matrix elements at higher orders through the following combinations, named effective Wilson coefficients [57],

$$\begin{aligned} C_7^{\text{eff}} &= \frac{4\pi}{\alpha_s} C_7 - \frac{1}{3} C_3 - \frac{4}{9} C_4 - \frac{20}{3} C_5 - \frac{80}{9} C_6, \\ C_9^{\text{eff}} &= \frac{4\pi}{\alpha_s} C_9 + Y(q^2), \\ C_{10}^{\text{eff}} &= \frac{4\pi}{\alpha_s} C_{10}, \end{aligned} \quad (3.4)$$

where the function $Y(q^2)$ is defined in eq. (B.5).

3.2 Theoretical formalism

3.2.1 $B_s \rightarrow \mu^+ \mu^-$

The rare decay $B_s \rightarrow \mu^+ \mu^-$ is one of the most powerful probes in the search for deviations from the SM. In the effective Hamiltonian of eq. (3.4), only the operator \mathcal{O}_{10} is relevant to this process and the branching ratio is given by [58–60]

$$\mathcal{B}(B_s \rightarrow \mu^+ \mu^-) = \frac{G_F^2 \alpha_e^2}{64\pi^3} m_{B_s}^3 f_{B_s}^2 |\lambda_t|^2 \tau_{B_s} \sqrt{1 - \frac{4m_\mu^2}{m_{B_s}^2}} \cdot \frac{4m_\mu^2}{m_{B_s}^2} \cdot |C_{10}^{\text{eff}}|^2, \quad (3.5)$$

where f_{B_s} is the B_s meson decay constant. Recently, a sizable width difference $\Delta\Gamma_s$ between the B_s mass eigenstates has been measured at the LHCb [63]

$$y_s \equiv \frac{\Gamma_s^L - \Gamma_s^H}{\Gamma_s^L + \Gamma_s^H} = \frac{\Delta\Gamma_s}{2\Gamma_s} = 0.088 \pm 0.014, \quad (3.6)$$

where Γ_s is the inverse of the B_s mean lifetime τ_{B_s} . Interestingly, it has been pointed out in ref. [61, 62] that the sizable width difference should be taken into account in the evaluation of the branching ratio to compare with its experimental measurement, thus the measured branching ratio should be the time-integrated one which reads

$$\bar{\mathcal{B}}(B_s \rightarrow \mu^+ \mu^-) = \left[\frac{1 + \mathcal{A}_{\Delta\Gamma} y_s}{1 - y_s^2} \right] \mathcal{B}(B_s \rightarrow \mu^+ \mu^-), \quad (3.7)$$

where the observable $\mathcal{A}_{\Delta\Gamma}$, equals to +1 in the SM, may vary in the interval $[-1, +1]$ in the presence of NP and can be extracted from time-dependent measurement of $B_s \rightarrow \mu^+ \mu^-$.

3.2.2 $\bar{B} \rightarrow \bar{K}^* l^+ l^-$

The $\bar{B} \rightarrow \bar{K}^* l^+ l^-$ decays are induced by the $b \rightarrow sl^+ l^-$ transition at quark level and provide constraints on the semileptonic operators $\mathcal{O}_{9,10}$. In this paper, we focus on the differential branching ratio, forward-backward asymmetry and longitudinal fraction at both the large and the low hadronic recoil, which can be built from transversity amplitudes

$$\begin{aligned} \frac{d\Gamma}{dq^2} &= |A_0^L|^2 + |A_\perp^L|^2 + |A_\parallel^L|^2 + (L \leftrightarrow R), \\ A_{\text{FB}} &= \frac{3\beta_l}{2} \frac{\text{Re}(A_\parallel^L A_\perp^{L*}) - \text{Re}(A_\parallel^R A_\perp^{R*})}{d\Gamma/dq^2}, \\ F_L &= \frac{|A_0^L|^2 + |A_0^R|^2}{d\Gamma/dq^2}, \end{aligned} \quad (3.8)$$

where q^2 is the dilepton invariant mass squared and $\beta_l = \sqrt{1 - 4m_l^2/q^2}$ is the phase space factor. After the first treatment by naive factorization [25], it has been shown that a systematic theoretical description using QCD factorization (QCDF) applies in the large hadronic recoil region $1 \text{ GeV}^2 \lesssim q^2 \ll 4m_c^2 \approx 7 \text{ GeV}^2$ [26, 27]. For the low recoil region $q^2 \gtrsim 15 \text{ GeV}^2$, an approach based on an operator product expansion in $1/m_b$ and in $1/\sqrt{q^2}$ with improved Isgur-Wise form factor relations has been developed [28, 64–67]. These theoretical treatments and the corresponding expressions of the transversity amplitudes $A_{\perp,\parallel,0}^{L,R}$ are shown in appendix B. It is noted that the observables $d\Gamma/dq^2$ and A_{FB} at low recoil only depend on the two combinations of Wilson coefficients ρ_1 and ρ_2 defined in eq. (B.9), while the F_L are independent of Wilson coefficients.

For the $7 \text{ GeV}^2 \lesssim q^2 \lesssim 15 \text{ GeV}^2$ region, the large quark-hadron duality violations caused by narrow $c\bar{c}$ resonances [68] and the hadronic backgrounds from $B \rightarrow K^*\psi^{(\prime)}$ make it difficult to give reliable theoretical predictions from the first principle. In the $q^2 \lesssim 1 \text{ GeV}^2$ region, the factorization formulae suffer from end-point divergences (at $q^2 \approx \Lambda_{\text{QCD}}^2$) [26, 27] and there could also be (unknown) resonance contributions from ρ or other mesons as discussed in ref. [69]. Additionally, theoretical predictions dependent largely on the Wilson coefficient C_7^{eff} , which is bounded more stringently by the $b \rightarrow s\gamma$ processes. Therefore, we do not include these two regions in our analysis.

3.3 Anomalous tqZ coupling effects

The effective tqZ vertices in eq. (2.1) affect the $b \rightarrow sl^+l^-$ processes through entering the bsZ -penguin diagram and result in the following effective Hamiltonian [24]

$$\mathcal{H}_{\text{eff}}^{\text{NP}} = -\frac{4G_F}{\sqrt{2}}\lambda_t\frac{\alpha_e}{2\pi\sin^2\theta_W}C^{\text{NP}}(\bar{s}\gamma_\mu P_L b)(\bar{l}\gamma^\mu P_L l), \quad (3.9)$$

or in the operator basis in eq. (3.3)

$$\mathcal{H}_{\text{eff}}^{\text{NP}} = -\frac{4G_F}{\sqrt{2}}\lambda_t\frac{\alpha_s}{4\pi\sin^2\theta_W}C^{\text{NP}}(\mathcal{O}_9 - \mathcal{O}_{10}). \quad (3.10)$$

The matching coefficient C^{NP} has been calculated in the unitary gauge with the modified minimal subtraction ($\overline{\text{MS}}$) scheme [24]. It is found that, besides the left-handed vector current $\bar{c}\gamma^\mu P_L t Z_\mu$ all the contributions from the tqZ anomalous interactions in the effective Lagrangian

eq. (2.1) can be safely neglected, then the coefficient reads

$$C^{\text{NP}} = -\frac{1}{8} \frac{V_{cs}^*}{V_{ts}^*} \left[\left(-x_t \ln \frac{m_W^2}{\mu^2} + \frac{3}{2} + x_t - x_t \ln x_t \right) X_{ct}^L + \mathcal{O} \left(\frac{m_c}{m_W} \right) X_{ct}^R \right], \quad (3.11)$$

with $x_t \equiv \bar{m}_t^2/m_W^2$. Compared with the SM case, the coefficient C^{NP} is enhanced by a large CKM factor V_{cs}^*/V_{ts}^* , which makes the $b \rightarrow sl^+l^-$ transitions sensitive to the anomalous tcZ coupling.

Normalized to the effective Hamiltonian eq. (3.1), the anomalous tcZ coupling effects result in the following deviations

$$\begin{aligned} C_9^{\text{eff}} \rightarrow \tilde{C}_9^{\text{eff}} &= C_9^{\text{eff}} + \frac{C^{\text{NP}}}{\sin^2 \theta_W} = +4.29 \left(1 + 17.3 |X_{ct}^L| e^{i(\theta_{ct}^L + \beta_s)} \right) + Y(q^2), \\ C_{10}^{\text{eff}} \rightarrow \tilde{C}_{10}^{\text{eff}} &= C_{10}^{\text{eff}} - \frac{C^{\text{NP}}}{\sin^2 \theta_W} = -4.22 \left(1 + 17.6 |X_{ct}^L| e^{i(\theta_{ct}^L + \beta_s)} \right), \end{aligned} \quad (3.12)$$

where the SM Wilson coefficients are the NNLL numerical values and the phase $\beta_s \approx 1.04^\circ$ can be obtained from its definition $\beta_s \equiv -\arg(-V_{cs}V_{cb}^*/V_{ts}V_{tb}^*)$. It is noted that, in the transversity amplitudes $A_{\perp,\parallel,0}^R$, the anomalous coupling only enters the combination $(C_9^{\text{eff}} + C_{10}^{\text{eff}})$ and their effects would be tiny.

For the $B_s \rightarrow \mu^+\mu^-$ decay in particular, the deviation of the Wilson coefficient C_{10}^{eff} also enters the observable $\mathcal{A}_{\Delta\Gamma}$ [61, 62],

$$\mathcal{A}_{\Delta\Gamma} = \cos \left[2 \arg \left(\frac{\tilde{C}_{10}^{\text{eff}}}{C_{10}^{\text{eff}}} \right) \right] = \cos \left[2 \arg \left(1 + 17.6 |X_{ct}^L| e^{i(\theta_{ct}^L + \beta_s)} \right) \right]. \quad (3.13)$$

This NP effects would result in a tiny suppression (up to 2%) on the branching ratio.

For the rare $t \rightarrow cZ$ decay mediated by anomalous tcZ coupling, the branching ratio has been calculated at NLO [70–74]. We shall follow the treatment of ref. [24] and only consider the LO results.

4 Numerical results and discussions

With the theoretical framework discussed in previous sections and the input parameters collected in table 1, we shall present our numerical results and discussions in this section.

G_F	$1.1663787 \times 10^{-5} \text{ GeV}^{-2}$	[75]	m_W	$(80.385 \pm 0.015) \text{ GeV}$	[75]
$\sin^2 \theta_W$	0.23146	[75]	m_Z	$(91.1876 \pm 0.0021) \text{ GeV}$	[75]
$\alpha_s(m_Z)$	0.1184 ± 0.0007	[75]	m_t^{pole}	$(173.18 \pm 0.94) \text{ GeV}$	[77]
$\alpha_e(m_Z)$	1/127.944	[75]	$m_c(m_c)$	$(1.275 \pm 0.025) \text{ GeV}$	[75]
$\alpha_e(m_b)$	1/133	[28]	$m_b(m_b)$	$(4.18 \pm 0.03) \text{ GeV}$	[75]
A	$0.812_{-0.022}^{+0.015}$	[76]	m_{K^*}	895.94 MeV	[75]
λ	$0.22543_{-0.00095}^{+0.00059}$	[76]	m_{B^0}	5279.58 MeV	[75]
$\bar{\rho}$	0.145 ± 0.027	[76]	m_{B_s}	5366.77 MeV	[75]
$\bar{\eta}$	0.343 ± 0.015	[76]	τ_{B^0}	$(1.519 \pm 0.007) \text{ ps}$	[75]
f_{B_s}	$(227.6 \pm 5.0) \text{ MeV}$	[78]	τ_{B_s}	$(1.466 \pm 0.031) \text{ ps}$	[75]
$\bar{\mathcal{B}}(B_s \rightarrow \mu^+ \mu^-) = (3.2_{-1.2}^{+1.5}) \times 10^{-9}$ ($\in [1.3, 5.8] \times 10^{-9}$ at 90% C.L.)					[46]

Table 1: The relevant input parameters and experimental data used in our numerical analysis.

4.1 The SM predictions

For the decay $\bar{B} \rightarrow \bar{K}^* \mu^+ \mu^-$, our SM predictions for the branching ratio $d\mathcal{B}/dq^2$, the forward-backward asymmetry A_{FB} and the longitudinal polarization fraction F_L with the available data from LHCb [44] are shown in figure 1. For the integrated observables, we take the ratio in eq. (3.8) after integrating its numerator and denominator separately. This definition agrees with the one used in the experimental measurements [28].

For the theoretical uncertainties, we follow closely the treatment of ref. [28]. At large recoil, we employ the naive factorization approach, therefore a real scale factor varying within $\pm 10\%$ is added to each of the transversity amplitudes $A_{\perp, \parallel, 0}^{L,R}$ in eq. (B.1) to account for the $\mathcal{O}(\alpha_s)$ and $\mathcal{O}(\Lambda/m_b)$ subleading QCDF corrections. Similarly, at low recoil, the $\mathcal{O}(\alpha_s \Lambda/m_b)$ subleading corrections to each of the transversity amplitudes $A_{\perp, \parallel, 0}^{L,R}$ in eq. (B.7) are estimated by real scale factors varying within $\pm 5\%$. For the uncertainties due to the $\mathcal{O}(\Lambda/m_b)$ subleading corrections to the improved Isgur-Wise relations and the $\mathcal{O}(m_{K^*}/m_B)$ neglected kinematical factors, three real scale factors with $\pm 20\%$ uncertainties are assigned to the κC_7^{eff} term for $A_{\perp, \parallel, 0}^{L,R}$ in eq. (B.7), respectively. We obtain the theoretical uncertainties by varying each of the input parameters and the real scale factors mentioned above within its respective range and adding the individual uncertainty in quadrature.

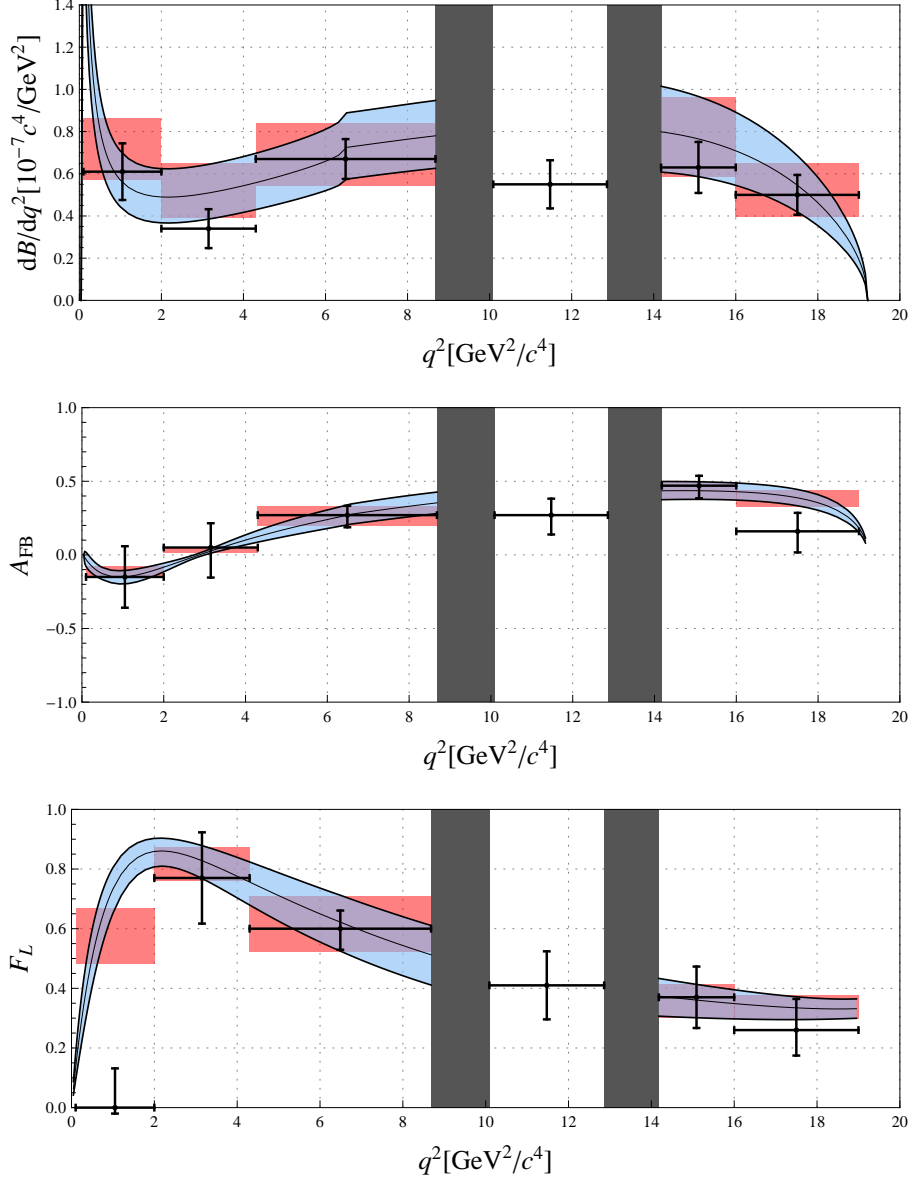


Figure 1: The SM predictions for the $d\mathcal{B}/dq^2$, A_{FB} and F_L with the theoretical uncertainties (the bands) versus the experimental measurements by LHCb [44]. The rate-averaged observables are indicated by the red regions.

From figure 1, it can be seen that the theoretical uncertainties for the branching ratio are about 30%, which mainly arise from the $B \rightarrow K^*$ form factors. However, in the angular observables forward-backward asymmetry and longitudinal fraction, these hadronic uncertainties cancel each other, which result in the relatively precise theoretical predictions.

With the theoretical uncertainties taken into account, the LHCb data are well consistent

with the SM predictions except the F_L in the lowest- q^2 bin $q^2 \in [0.10, 2.00]$ GeV². For this bin, it is noted that the recent LHCb preliminary result of the F_L (with $\mathcal{L} = 1 \text{ fb}^{-1}$) [45] deviates from their previous result [44] by about 2.5σ and is in agreement with the SM prediction.

For the $B_s \rightarrow \mu^+\mu^-$ decay, with the up-to-date input parameters listed in table 1, we obtain the SM prediction

$$\overline{\mathcal{B}}(B_s \rightarrow \mu^+\mu^-) = (3.71 \pm 0.24) \times 10^{-9}, \quad (4.1)$$

where the theoretical uncertainty is dominated by the decay constant f_{B_s} and the CKM matrix elements. As pointed out in ref. [61, 62], the correction in eq. (3.7) gives a 10% enhancement of the branching ratio (compared with the one without the effects of $B_s^0 - \bar{B}_s^0$ mixing). This value is in good agreement with the observed rate at the LHCb, which will put severe constraints on the anomalous tcZ coupling as seen in the following analysis.

4.2 Constraining anomalous tcZ coupling

In order to constrain the anomalous tcZ coupling, we consider the SM predictions with 2σ error bars and the experimental data with 1σ error bar. For the $\bar{B} \rightarrow \bar{K}^*\mu^+\mu^-$ decays, as discussed in subsection 3.2.2 and 4.1, the LHCb data [44] in the following four bins $q^2 \in [2.00, 4.30]$ GeV², $[4.30, 8.68]$ GeV², $[14.18, 16.00]$ GeV² and $[16.00, 19.00]$ GeV² are included in our analysis, which are also depicted in figure 1. For the decay $B_s \rightarrow \mu^+\mu^-$, we consider the recent LHCb measurements [46] listed in table 1.

The constraints on the anomalous coupling in the $|X_{ct}^L| - \theta_{ct}^L$ plane by the $d\mathcal{B}/dq^2$, A_{FB} , F_L and their combinations in the $\bar{B} \rightarrow \bar{K}^*\mu^+\mu^-$ decays are shown in figure 2. It can be seen that, the potentially large tcZ coupling effects are reflected in the stringent bound on its magnitude $|X_{ct}^L|$, which is currently dominated by the differential branching ratio. For a given value $|X_{ct}^L|$, the NP contribution is constructive to the SM one in the region $\theta_{ct}^L \approx 0^\circ$, whereas their interference becomes destructive in the region $\theta_{ct}^L \approx \pm 180^\circ$. Therefore, there are two favored solutions under the constraints of differential branching ratio in the $\theta_{ct}^L \approx \pm 180^\circ$ region. The solution with larger $|X_{ct}^L|$ corresponds to the case that the sign of $(C_9^{\text{eff}}, C_{10}^{\text{eff}})$ has been flipped by the anomalous coupling. This solution is also not consistent with the CMS bound as depicted in figure 2. For the forward-backward asymmetry and longitudinal fraction,

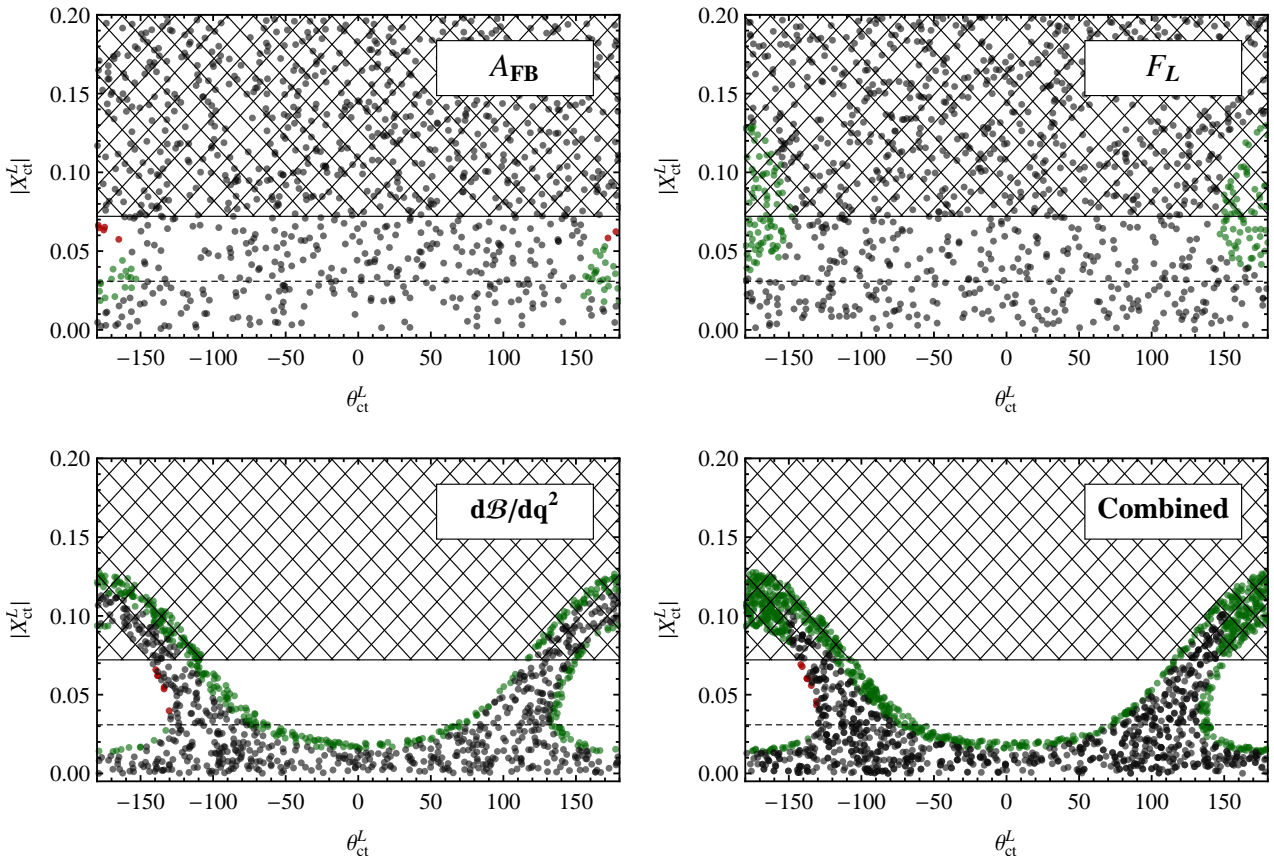


Figure 2: The allowed regions of the anomalous coupling $|X_{ct}^L|$ as a function of θ_{ct}^L under the constraints from $\bar{B} \rightarrow \bar{K}^* \mu^+ \mu^-$ distributions $d\mathcal{B}/dq^2$, A_{FB} and F_L and their combinations by using the LHCb data [44]. The allowed regions by the experimental data at large recoil (low recoil) are shown in red and black (green and black) points. Furthermore, the black points are allowed by all the data. The cross-hatched region are excluded by the CMS bound on $\mathcal{B}(t \rightarrow cZ)$ [9]. The ATLAS 5σ discovery potential at $\mathcal{L} = 10 \text{ fb}^{-1}$ [10, 11] is indicated by the dashed line.

they can not provide strong constraints on the anomalous coupling. However, the longitudinal fraction at large recoil excludes this sign-flipped solution. Exploiting the $\bar{B} \rightarrow \bar{K}^* \mu^+ \mu^-$ data, the constraints from the large recoil region are slightly more stringent than the ones from low recoil and comparable to the latter.

For the constraints on the anomalous tcZ coupling by the $B_s \rightarrow \mu^+ \mu^-$ decays, after considering the recent LHCb data [46], we update our previous results [24] at figure 3. It can be seen that, the interference structure between the SM and NP contributions manifested in the

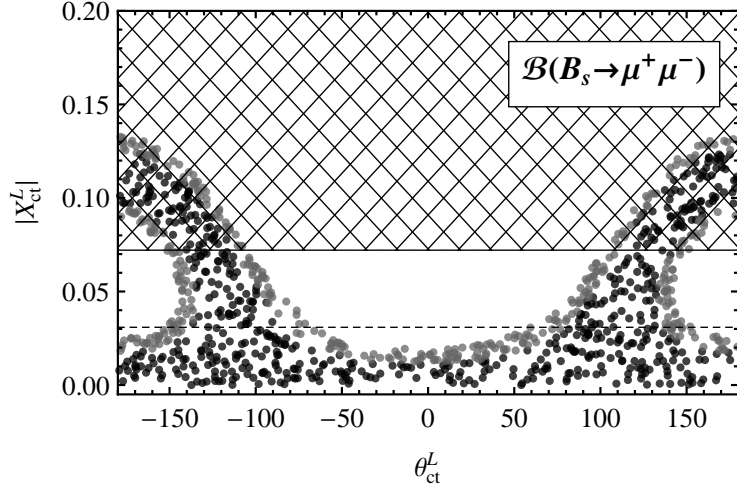


Figure 3: The upper bounds on the anomalous coupling $|X_{ct}^L|$ as a function of θ_{ct}^L , constrained by the $\bar{\mathcal{B}}(B_s \rightarrow \mu^+ \mu^-)$. The black (gray and black) region are the allowed parameter space obtained with 1σ experimental error bar (the experimental true value interval at 90% C.L.). The other captions are the same as in figure 2.

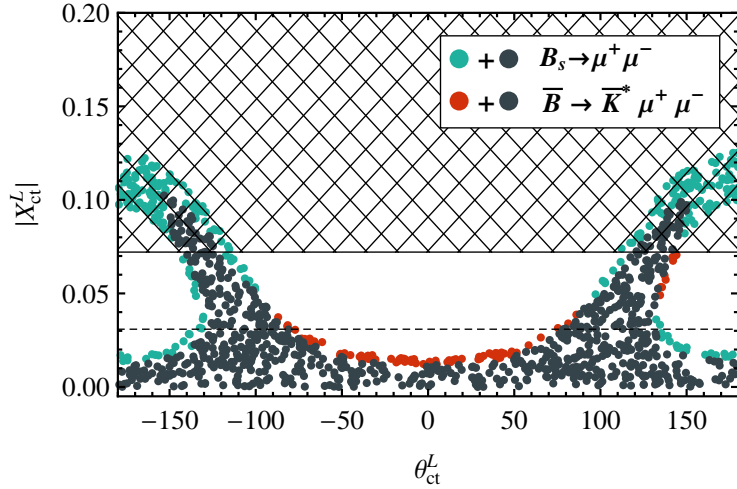


Figure 4: The combined upper bounds on the anomalous coupling $|X_{ct}^L|$ as a function of θ_{ct}^L . The allowed regions by the experimental data of $B_s \rightarrow \mu^+ \mu^-$ ($\bar{B} \rightarrow \bar{K}^* \mu^+ \mu^-$) are indicated by both green and black (red and black) points. Furthermore, the black points are allowed by all the data. The other captions are the same as in figure 2.

branching ratio is similar to the one in the $\bar{B} \rightarrow \bar{K}^* \mu^+ \mu^-$ decays. Compared with our previous constraints, since the experimental data of $B_s \rightarrow \mu^+ \mu^-$ are now double-bounded, it excludes parts of the parameter space in the destructive region $\theta_{ct}^L \approx \pm 180^\circ$ and leaves two solutions for

θ_{ct}^L	$ X_{ct}^L $ constrained from			our bound
	$B_s \rightarrow \mu^+\mu^-$	$\bar{B} \rightarrow \bar{K}^*\mu^+\mu^-$	CMS	$\mathcal{B}(t \rightarrow cZ)$
0°	< 0.012	< 0.015	< 0.072	$< 6.27 \times 10^{-5}$
180°	< 0.125	< 0.013	< 0.072	$< 0.75 \times 10^{-4}$
<i>general</i>	< 0.125	< 0.102	< 0.072	$< 4.85 \times 10^{-3}$

Table 2: The upper bounds on the magnitude $|X_{ct}^L|$ from the $\bar{B} \rightarrow \bar{K}^*\mu^+\mu^-$ and $B_s \rightarrow \mu^+\mu^-$ decays for some particular phases θ_{ct}^L . The corresponding predicted bounds on $\mathcal{B}(t \rightarrow cZ)$ are also given. The bounds in the fourth column are obtained from the direct search of the $t \rightarrow cZ$ decay at the CMS [9].

$|X_{ct}^L|$.

The combined constraints obtained after considering all the experimental data of both $B_s \rightarrow \mu^+\mu^-$ and $\bar{B} \rightarrow \bar{K}^*\mu^+\mu^-$ decays are shown in figure 4. In the parameter space of $(\theta_{ct}^L, |X_{ct}^L|)$, benefited from the angular observables, the $\bar{B} \rightarrow \bar{K}^*\mu^+\mu^-$ process excludes the regions corresponding to the sign-flipped solution. The constraints on the other part of the parameter space provided by these two decays are almost the same stringent. The detailed numerical results are listed in table 2. For general complex coupling X_{ct}^L , one can see that the predicted upper bound $\mathcal{B}(t \rightarrow cZ) < 4.85 \times 10^{-3}$ is compatible with the CMS direct bound $\mathcal{B}(t \rightarrow cZ) < 2.4 \times 10^{-3}$. For real coupling, the corresponding bound $\mathcal{B}(t \rightarrow cZ) < 6.3 \times 10^{-5}$ is below the CMS bound, but still of the same order as the 5σ discovery potential $\mathcal{B}(t \rightarrow cZ) \approx 4.4 \times 10^{-4}$ of the LHC with an integrated luminosity of 10 fb^{-1} .

5 Conclusions

In this paper, we have studied the effects of anomalous tcZ coupling in the $\bar{B} \rightarrow \bar{K}^*\mu^+\mu^-$ decays at both the large and the low hadronic recoil region. With the recent LHCb measurements of $B_s \rightarrow \mu^+\mu^-$, the combined constraints on the anomalous coupling X_{ct}^L from these two decays are derived. For general complex coupling, it is found that, the predicted upper limit of $\mathcal{B}(t \rightarrow cZ)$ is compatible with the CMS direct search. In particular, for real coupling, the corresponding limit is below the current CMS bound, but still stays in the accessible level of the LHC with

an integrated luminosity of 10 fb^{-1} .

It has been shown that, the $B_s \rightarrow \mu^+ \mu^-$ and $\bar{B} \rightarrow \bar{K}^* \mu^+ \mu^-$ decays can provide complementary information about the anomalous tcZ coupling, and therefore they are correlated with the rare $t \rightarrow cZ$ decays. With improved measurements from the LHCb and the future super-B factories, these interplays will be enhanced and complementary to the direct search for the FCNC transitions in top quark decays performed at the LHC CMS and ATLAS experiments.

Acknowledgements

The work was supported by the National Natural Science Foundation under contract Nos.11075059, 11225523 and 11221504. X.B.Yuan was also supported by CCNU-QLPL Innovation Fund (QLPL2011P01).

A The form factors

For the $\bar{B} \rightarrow \bar{K}^*$ transitions, we can use seven QCD form factors parameterize the matrix elements of $\mathcal{O}_{7,9,10}$ as ($q^\mu = p^\mu - k^\mu$) [79]

$$\begin{aligned}
\langle \bar{K}^*(k, \epsilon) | \bar{s} \gamma_\mu (1 - \gamma_5) b | \bar{B}(p) \rangle &= -i \epsilon_\mu^* (m_B + m_{K^*}) A_1(q^2) + i(2p - q)_\mu (\epsilon^* \cdot q) \frac{A_2(q^2)}{m_B + m_{K^*}} \\
&\quad + i q_\mu (\epsilon^* \cdot q) \frac{2m_{K^*}}{q^2} [A_3(q^2) - A_0(q^2)] + \epsilon_{\mu\nu\rho\sigma} \epsilon^{*\nu} p^\rho k^\sigma \frac{2V(q^2)}{m_B + m_{K^*}}, \\
\langle \bar{K}^*(k, \epsilon) | \bar{s} \sigma_{\mu\nu} q^\nu (1 + \gamma_5) b | \bar{B}(p) \rangle &= +T_3(q^2) (\epsilon^* \cdot q) \left[q_\mu - \frac{q^2}{m_B^2 - m_{K^*}^2} (2p - q)_\mu \right] \\
&\quad + i \epsilon_{\mu\nu\rho\sigma} \epsilon^{*\nu} p^\rho k^\sigma 2T_1(q^2) + T_2(q^2) [\epsilon_\mu^* (m_B^2 - m_{K^*}^2) - (\epsilon^* \cdot q) (2p - q)_\mu], \tag{A.1}
\end{aligned}$$

with

$$A_3(q^2) = \frac{m_B + m_{K^*}}{2m_{K^*}} A_1(q^2) - \frac{m_B - m_{K^*}}{2m_{K^*}} A_2(q^2) \tag{A.2}$$

and

$$A_0(0) = A_3(0), \quad T_1(0) = T_2(0). \tag{A.3}$$

At large recoil, after adopting the QCDF approach [80], these seven form factors can be reduced to two universal form factors, which are related to the form factors $V, A_{1,2}$ as [27, 81]

$$\xi_{\perp}(q^2) = \frac{m_B}{m_B + m_{K^*}} V(q^2), \quad \xi_{\parallel}(q^2) = \frac{m_B + m_{K^*}}{2E_{K^*}} A_1(q^2) - \frac{m_B - m_{K^*}}{m_B} A_2(q^2). \quad (\text{A.4})$$

At low recoil, the improved Isgur-Wise relations imply the vector and tensor form factors are connected as follows to leading order in $1/m_b$ [66, 67],

$$T_1(q^2) = \kappa V(q^2), \quad T_2(q^2) = \kappa A_1(q^2), \quad T_3(q^2) = \kappa A_2(q^2) \frac{m_B^2}{q^2}, \quad (\text{A.5})$$

with

$$\kappa = 1 - \frac{2\alpha_s}{3\pi} \ln\left(\frac{\mu}{m_b}\right), \quad (\text{A.6})$$

after neglecting subleading terms.

For the $B \rightarrow K^*$ form factors $V, A_{1,2}$, we adopt results of light-cone sum rule approach [79]

$$\begin{aligned} V(q^2) &= \frac{r_1}{1 - q^2/m_R^2} + \frac{r_2}{1 - q^2/m_{\text{fit}}^2}, & \text{with } r_1 = 0.923, r_2 = -0.511, \\ & & m_R = 5.32 \text{ GeV}, m_{\text{fit}}^2 = 49.40 \text{ GeV}^2, \\ A_1(q^2) &= \frac{r_2}{1 - q^2/m_{\text{fit}}^2}, & \text{with } r_2 = 0.290, m_{\text{fit}}^2 = 40.38 \text{ GeV}^2, \\ A_2(q^2) &= \frac{r_1}{1 - q^2/m_{\text{fit}}^2} + \frac{r_2}{(1 - q^2/m_{\text{fit}}^2)^2}, & \text{with } r_1 = -0.084, r_2 = 0.342, m_{\text{fit}}^2 = 52.00 \text{ GeV}^2. \end{aligned} \quad (\text{A.7})$$

Their relative uncertainties at $q^2 = 0$ are $\delta V(0) = \pm 11\%$, $\delta A_1(0) = \pm 12\%$ and $\delta A_2(0) = \pm 13\%$ after taking into account the uncertainties induced by the Gegenbauer moment a_{1,K^*} . For the $q^2 > 0$ region, the relative uncertainties are estimated to be the same as the ones at $q^2 = 0$.

B The transversity amplitudes

For the theoretical framework at the large and the low hadronic recoil region, we follow closely the ref. [28, 82] and recapitulate the relevant formulae in the following.

The transversity amplitudes at large recoil

At large recoil, application of QCDF yields the following transversity amplitudes [82]

$$\begin{aligned}
A_{\perp}^{L,R} &= +\sqrt{2}Nm_B(1-\hat{s}) \left[(\mathcal{C}_9 \mp \mathcal{C}_{10})\xi_{\perp} + \frac{2\hat{m}_b}{\hat{s}}\mathcal{T}_{\perp}^{\pm} \right], \\
A_{\parallel}^{L,R} &= -\sqrt{2}Nm_B(1-\hat{s}) \left[(\mathcal{C}_9 \mp \mathcal{C}_{10})\xi_{\perp} + \frac{2\hat{m}_b}{\hat{s}}\mathcal{T}_{\perp}^{\pm} \right], \\
A_0^{L,R} &= -\frac{Nm_B^2(1-\hat{s})^2}{2m_{K^*}\sqrt{\hat{s}}} \left[(\mathcal{C}_9 \mp \mathcal{C}_{10})\xi_{\parallel} - 2\hat{m}_b\mathcal{T}_{\parallel}^{\pm} \right],
\end{aligned} \tag{B.1}$$

where

$$\begin{aligned}
\hat{s} &= \frac{q^2}{m_B^2}, & \hat{m}_b &= \frac{m_b}{m_B}, & \hat{m}_{K^*} &= \frac{m_{K^*}}{m_B}, & N &= \left[\frac{G_F^2 \alpha_e^2 |\lambda_t|^2}{3 \cdot 2^{10} \pi^5} m_B \hat{s} \sqrt{\hat{\lambda} \beta_l} \right]^{1/2}, \\
\mathcal{C}_{9,10} &= \frac{4\pi}{\alpha_s} \mathcal{C}_{9,10}, & \hat{\lambda} &= 1 + \hat{m}_{K^*}^4 + \hat{s}^2 - 2(\hat{m}_{K^*}^2 + \hat{s} + \hat{s} \hat{m}_{K^*}^2).
\end{aligned} \tag{B.2}$$

The functions $\mathcal{T}_{\perp, \parallel}^{\pm}$ have been calculated at NLO [26, 27], which have the following general structure

$$\begin{aligned}
\mathcal{T}_a^{\pm} &= \mathcal{T}_a^{\pm(t)} + \hat{\lambda}_u \mathcal{T}_a^{(u)}, & \mathcal{T}_a^{\pm(t)} &= \mathcal{T}_a^{\pm(t),\text{LO}} + \frac{\alpha_s}{4\pi} \mathcal{T}_a^{\pm(t),\text{NLO}}, \\
\hat{\lambda}_u &= \frac{V_{ub}V_{us}^*}{V_{tb}V_{ts}^*}, & \mathcal{T}_a^{(u)} &= \mathcal{T}_a^{(u),\text{LO}} + \frac{\alpha_s}{4\pi} \mathcal{T}_a^{(u),\text{NLO}},
\end{aligned} \tag{B.3}$$

where $a = \perp, \parallel$. The LO formulae read

$$\begin{aligned}
\mathcal{T}_{\perp}^{\pm(t),\text{LO}} &= +\xi_{\perp} \left(C_7^{\text{eff}(0)} + \frac{\hat{s}}{2\hat{m}_b} Y^{(0)} \right), & \mathcal{T}_{\perp}^{(u),\text{LO}} &= +\xi_{\perp} \frac{\hat{s}}{2\hat{m}_b} Y^{(u)(0)}, \\
\mathcal{T}_{\parallel}^{-\perp(t),\text{LO}} &= -\xi_{\parallel} \left(C_7^{\text{eff}(0)} + \frac{1}{2\hat{m}_b} Y^{(0)} \right) + HS, & \mathcal{T}_{\parallel}^{(u),\text{LO}} &= -\xi_{\parallel} \frac{1}{2\hat{m}_b} Y^{(u)(0)} + HS,
\end{aligned} \tag{B.4}$$

where spectator effects are denoted by HS . The functions involving the one-loop contributions of four-quark operators are defined as

$$\begin{aligned}
Y(q^2) &= +h(q^2, m_c) \left(\frac{4}{3}C_1 + C_2 + 6C_3 + 60C_5 \right) - \frac{1}{2}h(q^2, m_b) \left(7C_3 + \frac{4}{3}C_4 + 76C_5 + \frac{64}{3}C_6 \right) \\
&\quad - \frac{1}{2}h(q^2, 0) \left(C_3 + \frac{4}{3}C_4 + 16C_5 + \frac{64}{3}C_6 \right) + \frac{4}{3}C_3 + \frac{64}{9}C_5 + \frac{64}{27}C_6, \\
Y^{(u)}(q^2) &= + \left(\frac{4}{3}C_1 + C_2 \right) [h(q^2, m_c) - h(q^2, 0)].
\end{aligned} \tag{B.5}$$

The basic fermion loop function reads

$$h(q^2, m_q) = -\frac{4}{9} \left(\ln \frac{m_q^2}{\mu^2} - \frac{2}{3} - z \right) - \frac{4}{9} (2+z) \sqrt{|z-1|} \times \begin{cases} \arctan \frac{1}{\sqrt{z-1}} & z > 1 \\ \ln \frac{1+\sqrt{1-z}}{\sqrt{z}} - \frac{i\pi}{2} & z \leq 1 \end{cases} \tag{B.6}$$

with $z = 4m_q^2/q^2$.

The transversity amplitudes at low recoil

At low recoil, with the improved Isgur-Wise form factor relations eq. (A.5), the transversity amplitudes can be written as [28]

$$\begin{aligned} A_{\perp}^{L,R} &= +i \left[(C_9^{\text{eff}} \mp C_{10}^{\text{eff}}) + \kappa \frac{2\hat{m}_b}{\hat{s}} C_7^{\text{eff}} \right] f_{\perp}, \\ A_{\parallel}^{L,R} &= -i \left[(C_9^{\text{eff}} \mp C_{10}^{\text{eff}}) + \kappa \frac{2\hat{m}_b}{\hat{s}} C_7^{\text{eff}} \right] f_{\parallel}, \\ A_0^{L,R} &= -i \left[(C_9^{\text{eff}} \mp C_{10}^{\text{eff}}) + \kappa \frac{2\hat{m}_b}{\hat{s}} C_7^{\text{eff}} \right] f_0, \end{aligned} \quad (\text{B.7})$$

with the definitions

$$\begin{aligned} N &= \left[\frac{G_F^2 \alpha_e^2 |\lambda_t|^2}{3 \cdot 2^{10} \pi^5} m_B \hat{s} \sqrt{\hat{\lambda}} \right]^{1/2}, & f_{\parallel} &= N m_B \sqrt{2} (1 + \hat{m}_{K^*}) A_1(q^2), \\ f_0 &= N m_B \frac{(1 - \hat{s} - \hat{m}_{K^*}^2)(1 + \hat{m}_{K^*})^2 A_1(q^2) - \hat{\lambda} A_2(q^2)}{2\hat{m}_{K^*}(1 + \hat{m}_{K^*})\sqrt{\hat{s}}}, & f_{\perp} &= N m_B \frac{\sqrt{2\hat{\lambda}}}{1 + \hat{m}_{K^*}} V(q^2). \end{aligned} \quad (\text{B.8})$$

Furthermore, we can define the two independent combinations of Wilson coefficients as [28]

$$\rho_1 \equiv \left| C_9^{\text{eff}} + \kappa \frac{2\hat{m}_b}{\hat{s}} C_7^{\text{eff}} \right|^2 + |C_{10}^{\text{eff}}|^2, \quad \rho_2 \equiv \text{Re} \left\{ \left(C_9^{\text{eff}} + \kappa \frac{2\hat{m}_b}{\hat{s}} C_7^{\text{eff}} \right) C_{10}^{\text{eff}*} \right\}. \quad (\text{B.9})$$

Then, at low recoil, the observables in eq. (3.8) turn to be the transparent forms

$$\frac{d\Gamma}{dq^2} = 2\rho_1 \times (f_0^2 + f_{\perp}^2 + f_{\parallel}^2), \quad A_{\text{FB}} = 3 \frac{\rho_2}{\rho_1} \times \frac{f_{\perp} f_{\parallel}}{f_0^2 + f_{\perp}^2 + f_{\parallel}^2}, \quad F_L = \frac{f_0^2}{f_0^2 + f_{\perp}^2 + f_{\parallel}^2}. \quad (\text{B.10})$$

References

- [1] S. L. Glashow, J. Iliopoulos and L. Maiani, Phys. Rev. D **2**, 1285 (1970).
- [2] G. Eilam, J. L. Hewett and A. Soni, Phys. Rev. D **44**, 1473 (1991) [Erratum-ibid. D **59**, 039901 (1999)].
- [3] J. A. Aguilar-Saavedra, Acta Phys. Polon. B **35**, 2695 (2004) [hep-ph/0409342].
- [4] M. Beneke, I. Efthymiopoulos, M. L. Mangano, J. Womersley, A. Ahmadov, G. Azuelos, U. Baur and A. Belyaev *et al.*, In *Geneva 1999, Standard model physics (and more) at the LHC* 419-529 [hep-ph/0003033].

- [5] W. Bernreuther, J. Phys. G **35**, 083001 (2008) [arXiv:0805.1333 [hep-ph]].
- [6] T. Aaltonen *et al.* [CDF Collaboration], Phys. Rev. Lett. **101**, 192002 (2008) [arXiv:0805.2109 [hep-ex]].
- [7] V. M. Abazov *et al.* [D0 Collaboration], Phys. Lett. B **701** (2011) 313 [arXiv:1103.4574 [hep-ex]].
- [8] G. Aad *et al.* [ATLAS Collaboration], JHEP **1209**, 139 (2012) [arXiv:1206.0257 [hep-ex]].
- [9] S. Chatrchyan *et al.* [CMS Collaboration], arXiv:1208.0957 [hep-ex].
- [10] J. Carvalho *et al.* [ATLAS Collaboration], Eur. Phys. J. C **52**, 999 (2007) [arXiv:0712.1127 [hep-ex]].
- [11] F. M. A. Veloso, CERN-THESIS-2008-106.
- [12] L. Benucci and A. Kyriakis, Nucl. Phys. Proc. Suppl. **177-178**, 258 (2008).
- [13] T. Han, K. Whisnant, B. L. Young and X. Zhang, Phys. Rev. D **55**, 7241 (1997) [hep-ph/9603247].
- [14] T. Han, K. Whisnant, B. L. Young and X. Zhang, Phys. Lett. B **385**, 311 (1996) [hep-ph/9606231].
- [15] F. Larios, M. A. Perez and C. P. Yuan, Phys. Lett. B **457**, 334 (1999) [hep-ph/9903394].
- [16] G. Burdman, M. C. Gonzalez-Garcia and S. F. Novaes, Phys. Rev. D **61**, 114016 (2000) [hep-ph/9906329].
- [17] P. J. Fox, Z. Ligeti, M. Papucci, G. Perez and M. D. Schwartz, Phys. Rev. D **78**, 054008 (2008) [arXiv:0704.1482 [hep-ph]].
- [18] J. P. Lee and K. Y. Lee, Phys. Rev. D **78**, 056004 (2008) [arXiv:0806.1389 [hep-ph]].
- [19] J. Drobnak, S. Fajfer and J. F. Kamenik, Phys. Lett. B **701**, 234 (2011) [arXiv:1102.4347 [hep-ph]].

- [20] J. Drobnak, S. Fajfer and J. F. Kamenik, Nucl. Phys. B **855**, 82 (2012) [arXiv:1109.2357 [hep-ph]].
- [21] B. Grzadkowski and M. Misiak, Phys. Rev. D **78**, 077501 (2008) [Erratum-ibid. D **84**, 059903 (2011)] [arXiv:0802.1413 [hep-ph]].
- [22] X. Yuan, Y. Hao and Y. Yang, Phys. Rev. D **83**, 013004 (2011) [arXiv:1010.1912 [hep-ph]].
- [23] X. -Q. Li, Y. -D. Yang and X. -B. Yuan, JHEP **1108**, 075 (2011) [arXiv:1105.0364 [hep-ph]].
- [24] X. -Q. Li, Y. -D. Yang and X. -B. Yuan, JHEP **1203**, 018 (2012) [arXiv:1112.2674 [hep-ph]].
- [25] A. Ali, P. Ball, L. T. Handoko and G. Hiller, Phys. Rev. D **61**, 074024 (2000) [hep-ph/9910221].
- [26] M. Beneke, T. Feldmann and D. Seidel, Nucl. Phys. B **612**, 25 (2001) [hep-ph/0106067].
- [27] M. Beneke, T. .Feldmann and D. Seidel, Eur. Phys. J. C **41**, 173 (2005) [hep-ph/0412400].
- [28] C. Bobeth, G. Hiller and D. van Dyk, JHEP **1007**, 098 (2010) [arXiv:1006.5013 [hep-ph]].
- [29] A. Khodjamirian, T. .Mannel, A. A. Pivovarov and Y. -M. Wang, JHEP **1009**, 089 (2010) [arXiv:1006.4945 [hep-ph]].
- [30] A. Khodjamirian, T. .Mannel and Y. -M. Wang, JHEP **1302**, 010 (2013) [arXiv:1211.0234 [hep-ph]].
- [31] F. Kruger and J. Matias, Phys. Rev. D **71**, 094009 (2005) [hep-ph/0502060].
- [32] Q. Chang, X. -Q. Li and Y. -D. Yang, JHEP **1004**, 052 (2010) [arXiv:1002.2758 [hep-ph]].
- [33] W. Altmannshofer, P. Paradisi and D. M. Straub, JHEP **1204**, 008 (2012) [arXiv:1111.1257 [hep-ph]].
- [34] R. -M. Wang, Y. -G. Xu, Y. -L. Wang and Y. -D. Yang, Phys. Rev. D **85**, 094004 (2012) [arXiv:1112.3174 [hep-ph]].

- [35] F. Beaujean, C. Bobeth, D. van Dyk and C. Wacker, JHEP **1208**, 030 (2012) [arXiv:1205.1838 [hep-ph]].
- [36] F. Kruger, L. M. Sehgal, N. Sinha and R. Sinha, Phys. Rev. D **61**, 114028 (2000) [Erratum-ibid. D **63**, 019901 (2001)] [hep-ph/9907386].
- [37] C. S. Kim, Y. G. Kim, C. -D. Lu and T. Morozumi, Phys. Rev. D **62**, 034013 (2000) [hep-ph/0001151].
- [38] S. Descotes-Genon, J. Matias, M. Ramon and J. Virto, arXiv: 1207.2753 [hep-ph];
- [39] J. Matias, F. Mescia, M. Ramon and J. Virto, arXiv: 1202.4266 [hep-ph].
- [40] J. P. Lees *et al.* [BABAR Collaboration], Phys. Rev. D **86**, 032012 (2012) [arXiv:1204.3933 [hep-ex]].
- [41] J. -T. Wei *et al.* [BELLE Collaboration], Phys. Rev. Lett. **103**, 171801 (2009) [arXiv:0904.0770 [hep-ex]].
- [42] T. Aaltonen *et al.* [CDF Collaboration], Phys. Rev. Lett. **108**, 081807 (2012) [arXiv:1108.0695 [hep-ex]].
- [43] Hideki Miyake for the CDF Collaboration, presented at ICHEP, July 2012, slides available at <http://indico.cern.ch/contributionDisplay.py?contribId=502&confId=181298>.
- [44] RAaaj *et al.* [LHCb Collaboration], Phys. Rev. Lett. **108**, 181806 (2012) [arXiv:1112.3515 [hep-ex]].
- [45] Abraham Gallas for the LHCb Collaboration, presented at ICHEP, July 2012, slides available at <http://indico.cern.ch/contributionDisplay.py?contribId=560&confId=181298>.
- [46] RAaaj *et al.* [LHCb Collaboration], arXiv:1211.2674 .
- [47] T. Appelquist and J. Carazzone, Phys. Rev. D **11**, 2856 (1975).
- [48] W. Buchmuller and D. Wyler, Nucl. Phys. B **268**, 621 (1986).
- [49] B. Grzadkowski, M. Iskrzynski, M. Misiak and J. Rosiek, JHEP **1010**, 085 (2010) [arXiv:1008.4884 [hep-ph]].

- [50] W. Hollik, J. I. Illana, S. Rigolin, C. Schappacher and D. Stockinger, Nucl. Phys. B **551**, 3 (1999) [Erratum-ibid. B **557**, 407 (1999)] [hep-ph/9812298].
- [51] J. A. Aguilar-Saavedra, Nucl. Phys. B **812**, 181 (2009) [arXiv:0811.3842 [hep-ph]].
- [52] K. G. Chetyrkin, M. Misiak and M. Munz, Phys. Lett. B **400**, 206 (1997) [Erratum-ibid. B **425**, 414 (1998)] [hep-ph/9612313].
- [53] C. Bobeth, M. Misiak and J. Urban, Nucl. Phys. B **574**, 291 (2000) [hep-ph/9910220].
- [54] P. Gambino, M. Gorbahn and U. Haisch, Nucl. Phys. B **673**, 238 (2003) [hep-ph/0306079].
- [55] M. Gorbahn and U. Haisch, Nucl. Phys. B **713**, 291 (2005) [hep-ph/0411071].
- [56] M. Gorbahn, U. Haisch and M. Misiak, Phys. Rev. Lett. **95**, 102004 (2005) [hep-ph/0504194].
- [57] A. J. Buras, M. Misiak, M. Munz and S. Pokorski, Nucl. Phys. B **424**, 374 (1994) [hep-ph/9311345].
- [58] G. Buchalla and A. J. Buras, Nucl. Phys. B **548**, 309 (1999) [hep-ph/9901288].
- [59] M. Misiak and J. Urban, Phys. Lett. B **451**, 161 (1999) [hep-ph/9901278].
- [60] A. J. Buras, J. Girrbach, D. Guadagnoli and G. Isidori, Eur. Phys. J. C **72**, 2172 (2012) [arXiv:1208.0934 [hep-ph]].
- [61] K. De Bruyn, R. Fleischer, R. Knegjens, P. Koppenburg, M. Merk, A. Pellegrino and N. Tuning, Phys. Rev. Lett. **109**, 041801 (2012) [arXiv:1204.1737 [hep-ph]].
- [62] K. De Bruyn, R. Fleischer, R. Knegjens, P. Koppenburg, M. Merk and N. Tuning, Phys. Rev. D **86**, 014027 (2012) [arXiv:1204.1735 [hep-ph]].
- [63] RAaaj *et al.* [LHCb Collaboration], LHCb-CONF-2012-002
- [64] G. Buchalla and G. Isidori, Nucl. Phys. B **525**, 333 (1998) [hep-ph/9801456].
- [65] M. Beylich, G. Buchalla and T. Feldmann, Eur. Phys. J. C **71**, 1635 (2011) [arXiv:1101.5118 [hep-ph]].

- [66] B. Grinstein and D. Pirjol, Phys. Lett. B **533**, 8 (2002) [hep-ph/0201298].
- [67] B. Grinstein and D. Pirjol, Phys. Rev. D **70**, 114005 (2004) [hep-ph/0404250].
- [68] M. Beneke, G. Buchalla, M. Neubert and C. T. Sachrajda, Eur. Phys. J. C **61**, 439 (2009) [arXiv:0902.4446 [hep-ph]].
- [69] W. Altmannshofer, P. Ball, A. Bharucha, A. J. Buras, D. M. Straub and M. Wick, JHEP **0901**, 019 (2009) [arXiv:0811.1214 [hep-ph]].
- [70] T. Han, R. D. Peccei and X. Zhang, Nucl. Phys. B **454**, 527 (1995) [hep-ph/9506461].
- [71] J. J. Zhang, C. S. Li, J. Gao, H. Zhang, Z. Li, C. -P. Yuan and T. -C. Yuan, Phys. Rev. Lett. **102**, 072001 (2009) [arXiv:0810.3889 [hep-ph]].
- [72] J. Drobnak, S. Fajfer and J. F. Kamenik, Phys. Rev. Lett. **104**, 252001 (2010) [arXiv:1004.0620 [hep-ph]].
- [73] J. J. Zhang, C. S. Li, J. Gao, H. X. Zhu, C. -P. Yuan and T. -C. Yuan, Phys. Rev. D **82**, 073005 (2010) [arXiv:1004.0898 [hep-ph]].
- [74] J. Drobnak, S. Fajfer and J. F. Kamenik, Phys. Rev. D **82**, 073016 (2010) [arXiv:1007.2551 [hep-ph]].
- [75] J. Beringer *et al.* [Particle Data Group Collaboration], Phys. Rev. D **86**, 010001 (2012).
- [76] J. Charles *et al.* [CKMfitter Group Collaboration], Eur. Phys. J. C **41**, 1 (2005) [hep-ph/0406184], updated results and plots available at: <http://ckmfitter.in2p3.fr>
- [77] T. Aaltonen *et al.* [CDF and D0 Collaborations], Phys. Rev. D **86**, 092003 (2012) [arXiv:1207.1069 [hep-ex]].
- [78] J. Laiho, E. Lunghi and R. S. Van de Water, Phys. Rev. D **81**, 034503 (2010) [arXiv:0910.2928 [hep-ph]]. Updates available on <http://latticeaverages.org/>.
- [79] P. Ball and R. Zwicky, Phys. Rev. D **71**, 014015 (2005) [hep-ph/0406232]. P. Ball and R. Zwicky, Phys. Rev. D **71**, 014029 (2005) [hep-ph/0412079].

- [80] J. Charles, A. Le Yaouanc, L. Oliver, O. Pene and J. C. Raynal, Phys. Rev. D **60**, 014001 (1999) [hep-ph/9812358].
- [81] M. Beneke and T. Feldmann, Nucl. Phys. B **592**, 3 (2001) [hep-ph/0008255].
- [82] C. Bobeth, G. Hiller and G. Piranishvili, JHEP **0807**, 106 (2008) [arXiv:0805.2525 [hep-ph]].